Electroweak gauge couplings at LEP

G. Bella

School of Physics and Astronomy,
Raymond and Beverly Sackler Faculty of Exact Sciences,
Tel Aviv University, 69978 Tel Aviv, Israel

Abstract

Using mainly W-pair events, the four LEP experiments have measured the charged current triple gauge boson WWγ, WWZ, couplings, $\Delta\kappa_\gamma$, Δg_1^z and λ. A precision of 0.02 – 0.04 has been obtained. Limits on the anomalous neutral current triple gauge boson VZγ (V=γ,Z) couplings, h_i^V, $i = 1, \ldots, 4$ have been obtained from Zγ final states. Similarly, Z-pair events have been used to extract limits on the VZZ (V=γ,Z) couplings, f_i^V, $i = 4, 5$. Anomalous quartic gauge boson (WW$\gamma\gamma$, WWZγ, ZZ$\gamma\gamma$) couplings, a_0^V, a_c^V (V=W,Z) and a_n have been constrained, using the $\nu\bar{\nu}\gamma\gamma$, q$\bar{\text{q}}\gamma\gamma$ and WWγ final states. All anomalous coupling results are consistent with the Standard Model value of 0.

1 Introduction

Gauge boson self couplings are direct consequence of the non-Abelian nature of the SU(2)$\times$U(1) electroweak theory. The Lagrangian of this theory contains triple and quartic gauge boson interaction terms involving W gauge bosons, namely WWγ, WWZ, WW$\gamma\gamma$, WWZγ, WWZZ and WWWW terms. The coefficients of these terms are called Charged Current (CC) Triple Gauge boson Couplings (TGCs) and Quartic Gauge boson Couplings (QGCs). Theories beyond the Standard Model (SM) very often predict anomalous contributions to the SM couplings, as well as new couplings associated with new terms in the Lagrangian. Some of these terms correspond to triple and quartic gauge vertices which do not involve W gauge bosons, such as Z$\gamma\gamma$, ZZγ, ZZZ and ZZ$\gamma\gamma$, and the corresponding coefficients are called Neutral Current (NC) TGCs or QGCs.

The experimental study of gauge boson couplings is an important tool to search for physics beyond the SM in a model independent way. Any result inconsistent with the SM predictions would be a clear evidence of new physics.

Low precision measurements of TGCs have been performed already at run I of the Tevatron using di-boson (Wγ, WW, WZ and ZZ) production. In 1996 the LEP e^+e^- collider at CERN entered into its second phase, LEP2, by doubling its beam energy to be above the WW production threshold. Table 1 lists the integrated luminosity per experiment collected at the different LEP2 centre-of-mass energies during the five years of LEP2 operation. In total, each experiment collected about 700 pb^{-1} corresponding to $\approx$10000 W-pairs. This large number of W-pairs, along with smaller number of events from other relevant processes has allowed to perform a significantly more precise measurement of TGCs. Unfortunately the effect of the SM QGCs at LEP2 is negligible, and only large anomalous QGC values can be excluded.

The measurements done by the four LEP experiments, ALEPH, DELPHI, L3 and OPAL, as well as the combined LEP results, are presented in this report.

Year	c.m. Energy (GeV)	Luminosity (pb^{-1})
1996	161.3	10
	172.1	10
1997	182.7	57
1998	188.6	183
1999	191.6	29
	195.5	76
	199.5	77
	201.6	38
2000	204.9	82
	206.6	137

Table 1: Centre-of-mass energies and approximate integrated luminosity values for the data taken at LEP2. The exact luminosity values vary between the different analyses. In year 2000 the centre-of-mass energy was varied between 202 and 209 GeV and the quoted energies are mean values.

2 Charged Current TGCs

2.1 Theoretical Background

The most general expression for the effective Lagrangian describing the WWV vertex (V=γ,Z) has seven terms [1]. Three terms, with the couplings g_1^V, κ_V and λ_V conserve both charge conjugation, C, and parity, P. Another term, with the coupling g_5^V, violates both C and P, thus conserving their product, CP. The other three terms violate CP, one of them, with the coupling g_4^V, violates only C, and the other two terms, $\hat{\kappa}_V$ and $\hat{\lambda}_V$ violate only P. In the SM g_1^V=κ_V=1 and all other couplings vanish. Hence, Δg_1^V=g_1^V-1, $\Delta\kappa_V$=κ_V-1 and all other couplings are called anomalous couplings.

Some of the couplings for V=γ are related to some electromagnetic properties of the W Boson. The W charge is eg_1^γ, the magnetic dipole moment is $-e(g_1^\gamma + \kappa_\gamma + \lambda_\gamma)/2M_\mathrm{W}$, the electric quadrupole moment is $-e(\kappa_\gamma - \lambda_\gamma)/{M_\mathrm{W}}^2$, the electric dipole moment is $-e(\hat{\kappa}_\gamma + \hat{\lambda}_\gamma)/2M_\mathrm{W}$, and the magnetic quadrupole moment is $-e(\hat{\kappa}_\gamma - \hat{\lambda}_\gamma)/{M_\mathrm{W}}^2$.

It would be prohibitively too complicated to make a simultaneous measurement of all 14 couplings. Instead, each one of them can be separately determined, assuming that all other couplings vanish. An alternative approach is to reduce the number of couplings using constraints which are motivated from theory or measurement done at lower energies. Requiring QED gauge invariance constrains g_1^γ to be 1, and g_5^γ to be zero. Custodial SU(2)$\times$U(1) symmetry is needed to constrain the electroweak parameter ρ to the experimental value of 1. From this symmetry, the following relations are obtained [1],

$$\begin{aligned} \Delta\kappa_\mathrm{z} &= \Delta g_1^\mathrm{z} - \Delta\kappa_\gamma \tan^2\theta_w, & \lambda_\mathrm{z} &= \lambda_\gamma, \\ \hat{\kappa}_\mathrm{z} &= -\hat{\kappa}_\gamma \tan^2\theta_w, & \hat{\lambda}_\mathrm{z} &= \hat{\lambda}_\gamma. \end{aligned} \quad (1)$$

With these constraints, only eight couplings are left, four of them are CP conserving:

Δg_1^z, $\Delta\kappa_\gamma$, λ_γ and g_5^z. The other four couplings are CP violating: $\hat{\kappa}_z$, $\hat{\lambda}_z$, g_4^γ and g_4^z. The three C- and P-conserving couplings, Δg_1^z, $\Delta\kappa_\gamma$ and $\lambda\equiv\lambda_\gamma$ have been addressed by most of the analyses.

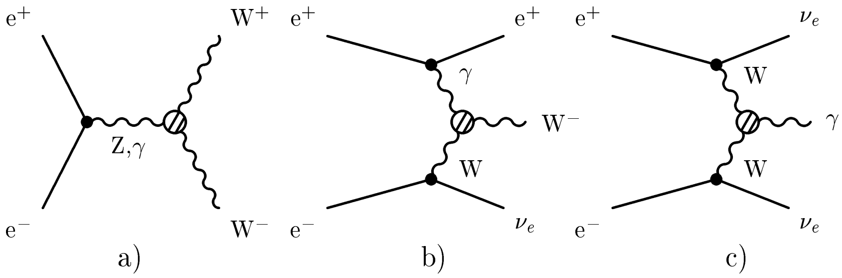

Figure 1: *Feynman diagrams of LEP2 processes with charged current triple gauge vertices.*

The TGC study at LEP [2] has been performed using the following three precesses:

- W-pair production, $e^+e^-\to W^+W^-$ (Fig. 1a), where the W-pair is produced via a virtual s-channel photon or Z. Hence, this process is sensitive to WWγ and WWZ couplings. This process is, by far, the most sensitive one to TGCs.
- Single W production, $e^+e^-\to We\overline{\nu}_e$ (Fig. 1b), where the electron[1] escapes undetected into the beam-pipe, leaving a quasi-real photon which interacts with a virtual W produced by the second incoming electron. This process is sensitive only to the WWγ couplings, but the large background from W-pairs does not allow to study the WWγ couplings independent of the WWZ ones. This process is less sensitive to TGCs than the W-pair production, but it still helps to constrain positive $\Delta\kappa_\gamma$ values.
- Single photon production, $e^+e^-\to\nu\overline{\nu}\gamma$ (Fig. 1c), where the photon is produced by a fusion of two virtual W bosons produced by the incoming electrons. This process clearly depends on the WWγ couplings only, without any WWZ-dependent background, so unlike the other two processes, it allows an independent study of the WWγ couplings, however with low sensitivity.

It is interesting to note that in the first process, both W bosons are real, whereas in the second process one W is real and one is virtual, and in the third process both W bosons are virtual. Each of these processes also gets contributions from diagrams which do not include the triple gauge vertex. Therefore, the total and differential cross-sections have a second order polynomial dependence on the TGCs.

Since the total cross-section depends on the TGCs, the total event rate in each process can be used to constrain the TGC values. However, the W-pair event rate as function of the TGCs has a minimum near the SM TGC values and the sensitivity is reduced. A similar situation occurs also for the λ_γ coupling for single W and single γ event rates. Therefore, the angular distributions have to be used in addition to the total event rates.

[1]In this report, the charge conjugate states are included and the word electron refers also to positron.

In W-pair and single W events, the sensitivity to anomalous couplings is not only in the W production angle, but also in the W polarisation state which can be probed by the W decay angles.

2.2 TGC Measurement from W-Pairs

W-pair events are observed in three different final states.

- $W^+W^- \rightarrow q\overline{q}\ell\overline{\nu}_\ell$, with a branching fraction of 43.9%, has a signature of two jets, an isolated charged lepton and a missing momentum. These events are selected with an efficiency varying between 70% ($q\overline{q}\tau\overline{\nu}_\tau$) and 90% ($q\overline{q}e\overline{\nu}_e$ and $q\overline{q}\mu\overline{\nu}_\mu$) and a typical purity of 90%. To study the angular distributions, the events have to be reconstructed. For this final state the event reconstruction is relatively simple.

- $W^+W^- \rightarrow q\overline{q}q\overline{q}$, with a branching fraction of 45.6%, has a signature of four jets. The background is mainly from $e^+e^- \rightarrow q\overline{q}$ events with final state radiation of two gluons or a quark-antiquark pair. The selection efficiency is ≈90% with a typical purity of 80%. There are three possible ways to associate the four jets into the parent W-bosons. Using the jet kinematic variables, the correct association can be achieved in ≈70% of the events. It is further needed to distinguish between the positive and negative W. This is done using a jet-charge technique and the correct charge is assigned in ≈70% of the events with correct jet pairing. The significant fraction of events with incorrect jet pairing or charge misassignment leads to a deterioration of the sensitivity in this channel with respect to the $q\overline{q}\ell\overline{\nu}_\ell$ events.

- $W^+W^- \rightarrow \ell\overline{\nu}_\ell\overline{\ell}\nu_\ell$, with a branching fraction of 10.5%, has a signature of two acollinear leptons. The selection efficiency for these events vary between 60% and 80% with a purity ≈90%. However, only those events not including tau leptons (4/9 of the whole sample) can be reconstructed. In these events the kinematic variables of the two unobserved neutrinos are obtained from the requirement of energy-momentum conservation and W mass constraint on both W bosons, leading to two solutions. This ambiguity, together with the low branching fraction of these events, make this channel less sensitive than $q\overline{q}\ell\overline{\nu}_\ell$.

The selected W pairs have been used to measure the total W-pair cross-section [2]. For this analysis, no event reconstruction is needed. The measurements of the four LEP experiments have been combined, accounting for common systematic errors, and the results are displayed in Fig. 2. The measured values agree with the theoretical prediction of the YFSWW [3] and RacoonWW [4] Monte Carlo programs which include the most complete $\mathcal{O}(\alpha)$ corrections. The 0.5% uncertainty in this prediction is represented in Fig. 2 by the width of the theoretical band. For a better check of this agreement between the measurements and theory, the ratio between the experimental and theoretical cross-section is calculated for each centre-of-mass energy. Averaging these ratios over all energy points, accounting for common systematic errors, yields a value of 0.997 ± 0.010.

The dashed and dotted lines in Fig. 2 represent the expected cross-section in the case where the WWZ or both WWZ and WWγ vertices are missing. These lines are far

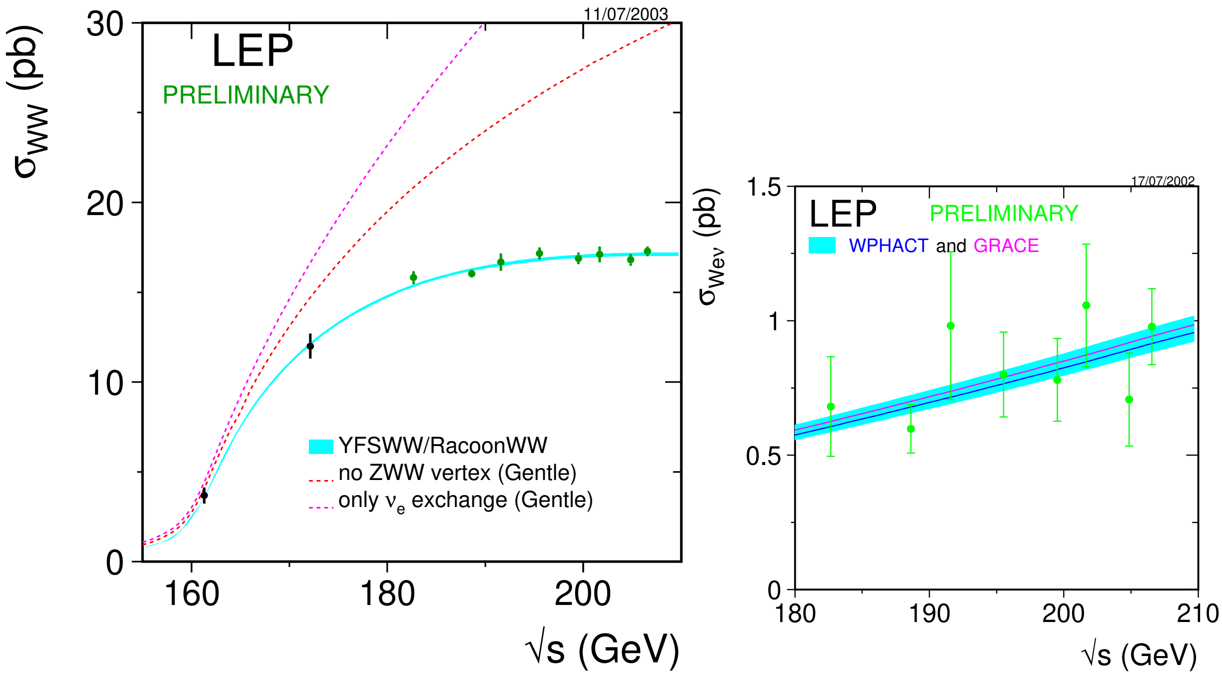

Figure 2: *LEP combined total cross-section for W-pair (left plot) and single W (right plot) production*

above the data points, demonstrating the need for TGCs. Constraints on TGCs obtained from the total event rate have been included in the final TGC determination, but as was mentioned above, the sensitivity from the W-pair angular distributions is far better.

Fig. 3 [5] shows the measured distribution of the W-pair production and decay angles for the $q\bar{q}\ell\bar{\nu}_\ell$ channel, along with the Monte Carlo distributions for the SM and for anomalous coupling $\lambda=\pm0.5$. The largest sensitivity is observed in the distribution of $\cos\theta$, the angle of the outgoing W^- with respect to the incoming e^-. A smaller sensitivity is observed in the other distributions of the decay angles of the fermion (anti-fermion) from the W^- (W^+) in the parent W rest-frame with respect to the W flight direction. However, there is also sensitivity in the correlations between these five angles.

To extract all the TGC information from the five-dimensional angular distribution, DELPHI and L3 are using binned maximum likelihood fit in the five-dimensional angular space, whereas ALEPH and OPAL are using the Optimal Observable method.

The systematic errors to the TGC measurement originate from uncertainties in the hadronisation model, $\mathcal{O}(\alpha)$ correction, background, detector simulation, initial and final state radiation, the centre-of-mass energy and W mass used in the kinematic fits, Monte Carlo statistics and final state interactions in $q\bar{q}q\bar{q}$ events, namely Bose-Einstein correlations and colour reconnection. In the total event rate analysis, also the uncertainties in the theoretical cross-section calculation and in the luminosity measurement are considered. The overall systematic uncertainty is around 50-70% of the statistical error, varying between the different experiments and anomalous couplings. In combining the results of the four experiments, the contributions to the systematic errors from hadronisation, $\mathcal{O}(\alpha)$ correction, final state interactions and theoretical cross-section are taken to be fully correlated between the LEP experiments.

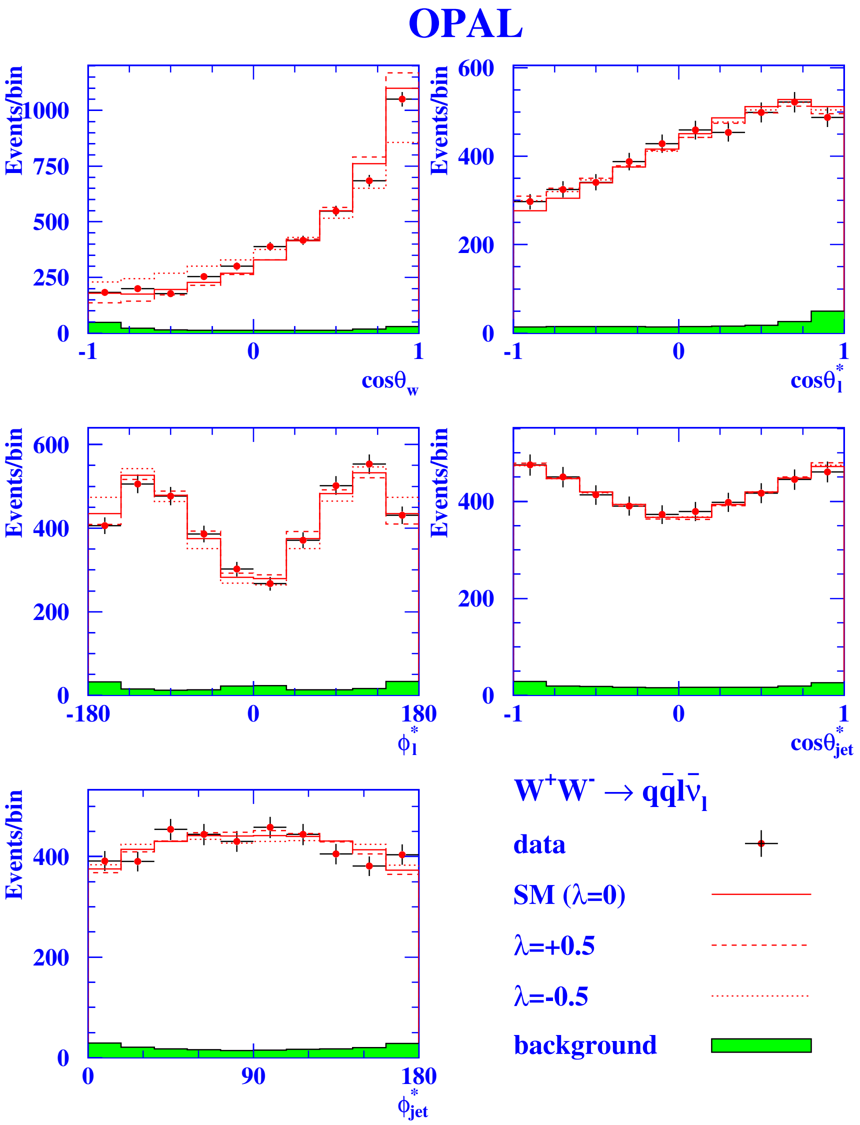

Figure 3: *Angular distributions of* $\mathrm{W^+W^-}\!\to\!\mathrm{q\overline{q}}\ell\overline{\nu}_\ell$ *events*

2.3 TGC Measurement from Single W Events

In single W events, only the W decay products are visible in the detector. For leptonic W decays, a single lepton is observed with a large missing momentum. The efficiency to select these events is about 40-60% with a purity varying between the different analyses from 45% to 80%. For hadronic W decays, two jets are observed with missing momentum, and the efficiency and purity vary in the ranges 40-60% and 45-80% respectively.

The TGC sensitivity for this process is primarily in the total event rate. Fig. 2 [2] shows the LEP combined cross-section measurement along with the theoretical expectation. In addition, some analyses are using also the lepton energy and polar angle, the angle between the two reconstructed jets and their total transverse momentum. Fig. 4 shows the ALEPH log-likelihood curves[2] from their single W analysis along with the corresponding curves from the other processes [6]. The contribution of the single W process is significant only for $\Delta\kappa_\gamma$. The overall log-likelihood is obtained by summing up the log-likelihood functions from the three different sources.

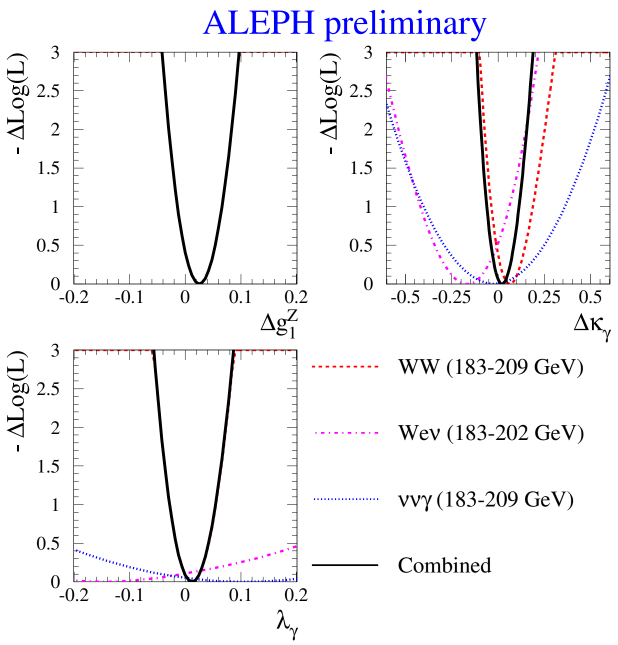

Figure 4: *ALEPH Log-likelihood curves for charged current TGCs from different processes*

2.4 TGC Measurement from Single Gamma Events

In single gamma events only the photon is visible in the detector. Besides the total event rate, the photon energy and polar angle distributions are used to extract the TGC log-likelihood curves, like the ones obtained by ALEPH and displayed in Fig. 4 [6]. This process, as mentioned already before, has a very low sensitivity, however the results obtained for the WWγ couplings are completely independent of any assumptions concerning the WWZ couplings.

2.5 Combined Charged Current TGC Results

The log-likelihood from the four LEP experiments for Δg_1^z, λ_γ and $\Delta\kappa_\gamma$ are shown in Fig. 5 [2]. Also shown are the combined curves and the numerical results. The results for the couplings are correlated, as can be seen from the contour plots in Fig. 5 which are

[2]In each log-likelihood plot throughout this report, the plotted function is $-\Delta \log L$ which is obtained by subtracting from $-\log L$ its minimum value. All other couplings are fixed at their SM values.

obtained by allowing two couplings to vary in the fit, fixing all other couplings at their SM values.

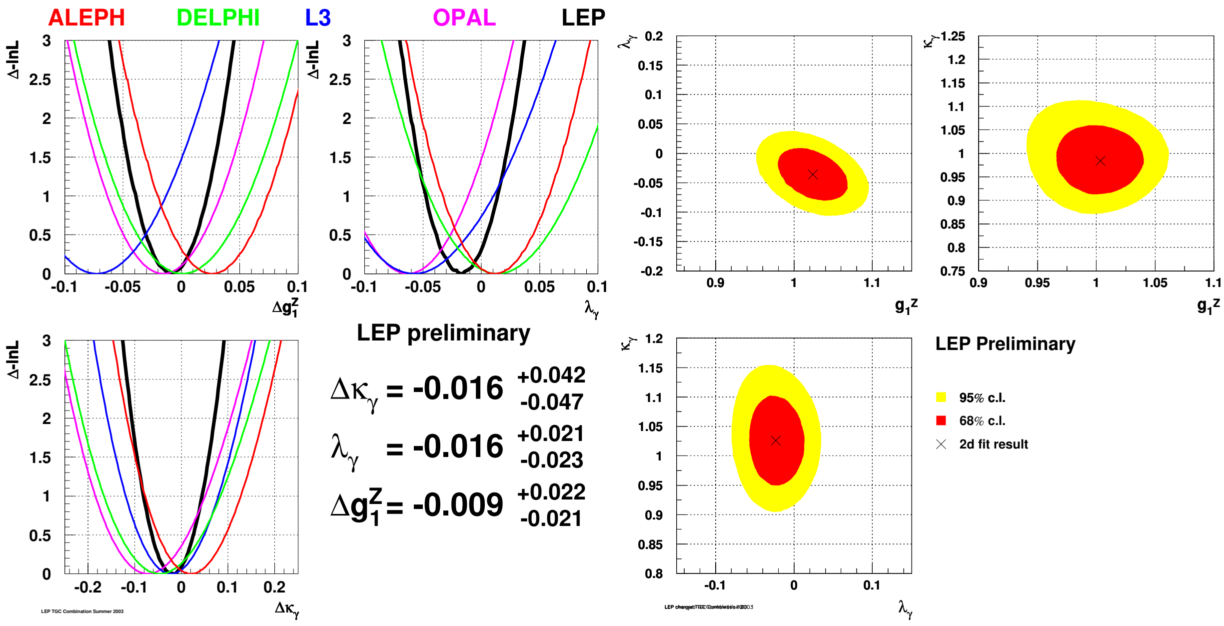

Figure 5: *LEP charged current TGC results: log-likelihood curves obtained from single parameter fits (left plots), and 68% and 95% c.l. contours obtained from two-parameter fits (right plots)*

2.6 Other Charged Current TGC Results

The ALEPH collaboration [6] has measured the real and imaginary parts of all 14 couplings without using the relations (2). Each value has been obtained, assuming that all other couplings (real and imaginary parts) vanish. OPAL [7] has employed the spin density method to measure the CP violating couplings $\hat{\kappa}_z$, $\hat{\lambda}_z$ and g_4^z, using the relations (2), and assuming also $g_4^z = g_4^\gamma$. All results are consistent with the SM.

3 Neutral Current TGCs

The main processes used at LEP2 to constrain neutral current TGCs are $e^+e^- \to Z\gamma$ and $e^+e^- \to ZZ$. The relevant Feynman diagrams for these processes are plotted in Fig. 6. The diagram in Fig. 6a is the SM one, whereas the diagram in Fig. 6b is due to a non-SM effective Lagrangian with triple neutral gauge boson, ZZZ, γZZ and $\gamma\gamma$Z interactions. The most general Lagrangian of this kind contains 15 CP-conserving and 29 CP-violating terms [8]. However, in Zγ and Z-pair events, the outgoing gauge bosons are produced on their mass shell, and due to Bose-statistics, the number of independent Lagrangian terms (and couplings) in this case reduces to 12 [9].

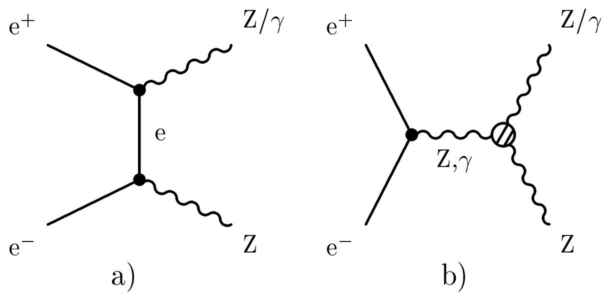

Figure 6: *Feynman diagrams of Z-pair or Zγ production. Diagram b does not exist in the SM.*

3.1 Zγ Production

The relevant triple gauge boson vertices for this process are $\gamma^*\mathrm{Z}\gamma$ and $Z^*\mathrm{Z}\gamma$, where γ^* and Z^* refer to the virtual gauge boson exchanged in the s-channel. For each of these vertices there are four possible terms in the Lagrangian, corresponding to four couplings, h_i^V, $i = 1, \ldots, 4$, $V = \gamma$,Z. The couplings h_1^V and h_2^V are CP-violating, whereas h_3^V and h_4^V are CP-conserving.

The LEP experiments have looked at Zγ events with $\mathrm{Z}\to\mathrm{q\bar{q}}$ and $\mathrm{Z}\to\nu\bar{\nu}$. For $\mathrm{Z}\to\mathrm{q\bar{q}}$ the signature is two jets with invariant mass consistent with M_Z along with an energetic and isolated photon. The photon is required to be in the central part of the detector in order to suppress the SM background from initial state radiation. The background from final state radiation is suppressed by the isolation requirement. For $\mathrm{Z}\to\nu\bar{\nu}$, only the photon is observed and it has to be in the central part of the detector and with energy such that the recoil mass of the event has to be consistent with M_Z. For both channels, the total event rate as well as some differential distributions are used to extract the TGC limits. Fig. 7 shows, for example, the distribution of the Z decay angle in its rest-frame with respect to the Z direction of flight, as measured by DELPHI [10], along with the Monte Carlo expectation for the SM case and for $h_3^\gamma = \pm 0.2$.

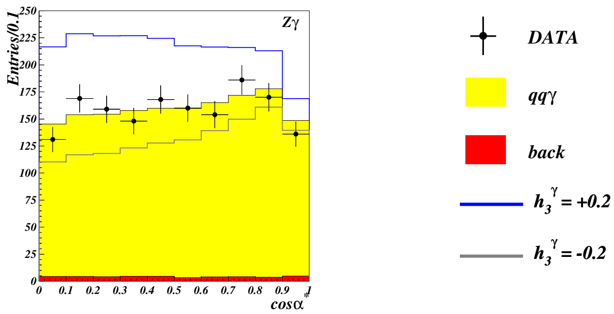

Figure 7: *DELPHI distribution of Z decay angle*

The log-likelihood curves from the four LEP experiments and the LEP combined curves are shown in Fig. 8 [2]. The 95% c.l. limits are listed in Table 2. Also two-parameter fit have been performed and the LEP combined contour plots are shown in Fig. 9 [2].

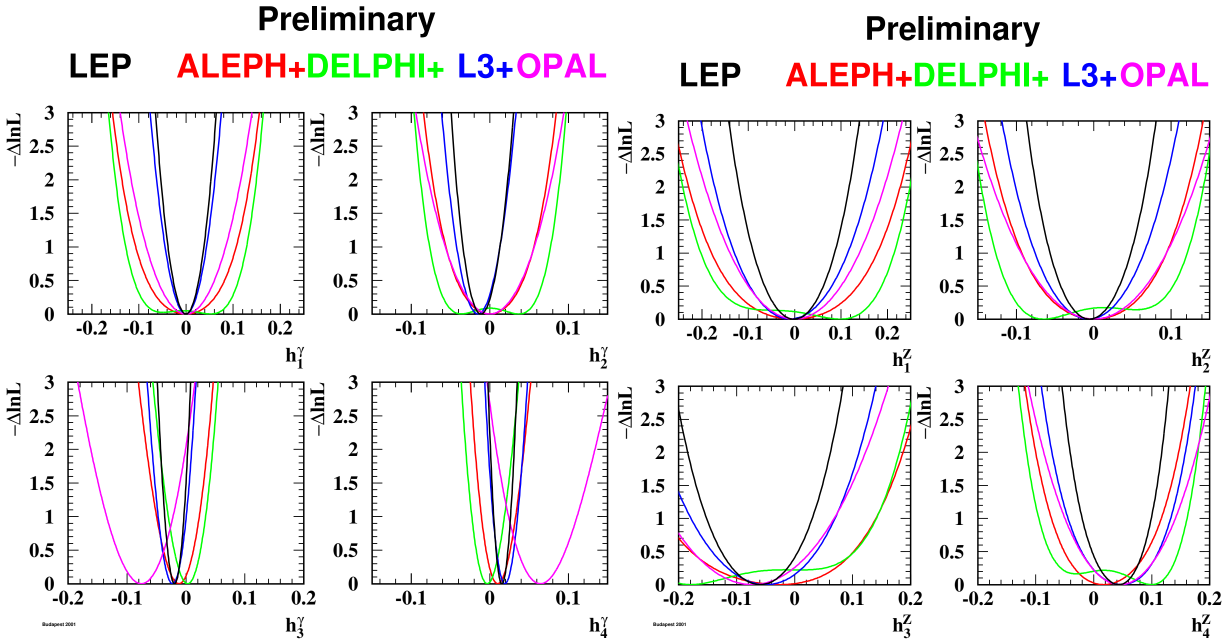

Figure 8: *LEP Log-likelihood curves for the h_i couplings*

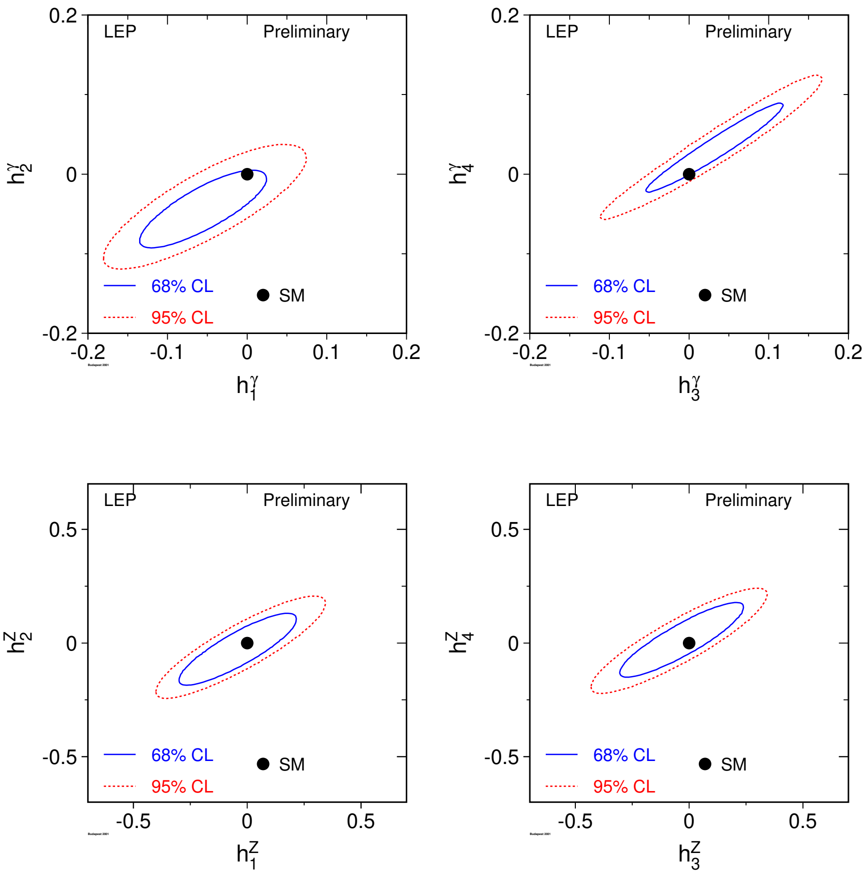

Figure 9: *68% and 95% c.l. contours obtained from two-parameter fits to the combined LEP $Z\gamma$ data*

$\gamma^*Z\gamma$ Couplings	$Z^*Z\gamma$ Couplings	γ^*ZZ Couplings	Z^*ZZ Couplings
$-0.056 < h_1^\gamma < 0.055$	$-0.13 < h_1^Z < 0.13$	$-0.17 < f_4^\gamma < 0.19$	$-0.30 < f_4^Z < 0.30$
$-0.045 < h_2^\gamma < 0.025$	$-0.078 < h_2^Z < 0.071$	$-0.32 < f_5^\gamma < 0.36$	$-0.34 < f_5^Z < 0.38$
$-0.049 < h_3^\gamma < -0.008$	$-0.20 < h_3^Z < 0.07$		
$-0.002 < h_4^\gamma < 0.034$	$-0.05 < h_4^Z < 0.12$		

Table 2: Combined LEP2 95% c.l. limits on neutral current TGCs

3.2 Z-pair Production

The relevant triple gauge boson vertices for this process are γ^*ZZ and Z^*ZZ, and for each one of them, there are two possible terms in the Lagrangian, corresponding to two couplings, f_4^V, f_5^V, $V = \gamma$,Z. The term with f_4^V violates CP whereas f_5^V conserves CP.

Z-pair production is interesting not only for the study of anomalous couplings, since it consists an almost irreducible background for the Higgs boson search in the case where $M_H \approx M_Z$. The LEP experiments have selected Z-pair events using all decay channels, except, of course, for those invisible events where both Z bosons decay into $\nu\overline{\nu}$. Table 3 lists the various decay channels, along with their branching fractions, and typical values of the selection efficiency and purity. The channels with highest background are those with the same final state topology as for W-pairs.

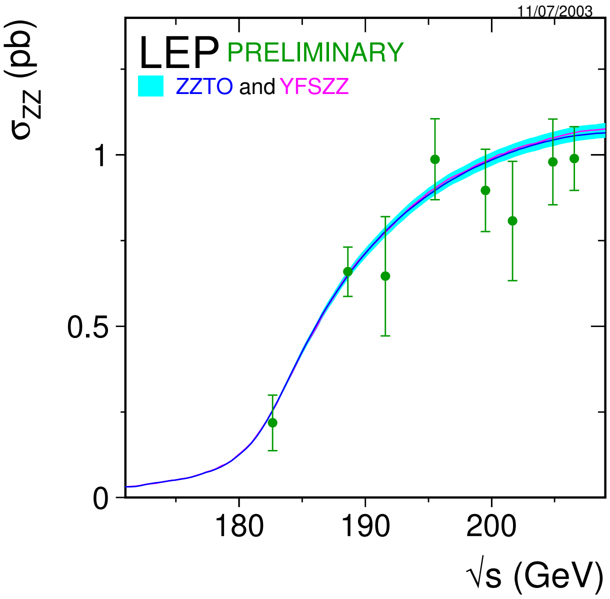

Figure 10: *LEP combined total Z-pair cross-section*

The LEP combined total Z-pair cross-section is plotted in Fig. 10 [2], along with the SM prediction. A nice agreement is obtained between the data points and the theoretical curves, which does not leave much room for any non-SM contribution.

For the TGC study, the total event rate, as well as angular distributions are used. Fig. 11 shows the log-likelihood curves from the four LEP experiments and the LEP combined curves. The 95% c.l. limits are listed in Table 2. The contour plots obtained in some two-parameter fits are also shown in Fig. 11.

Final state	Fraction	Efficiency	Purity
$q\bar{q}q\bar{q}$	49%	30%	(15-30)%
$q\bar{q}\nu\bar{\nu}$	28%	30%	60%
$q\bar{q}\ell^+\ell^-$	14%	(50-80)%	(80-90)%
$\ell^+\ell^-\nu\bar{\nu}$	4%	30%	(45-55)%
$\ell^+\ell^-\ell^+\ell^-$	1%	(40-60)%	(60-80)%

Table 3: Z-pair final states with their branching fractions, selection efficiencies and purities

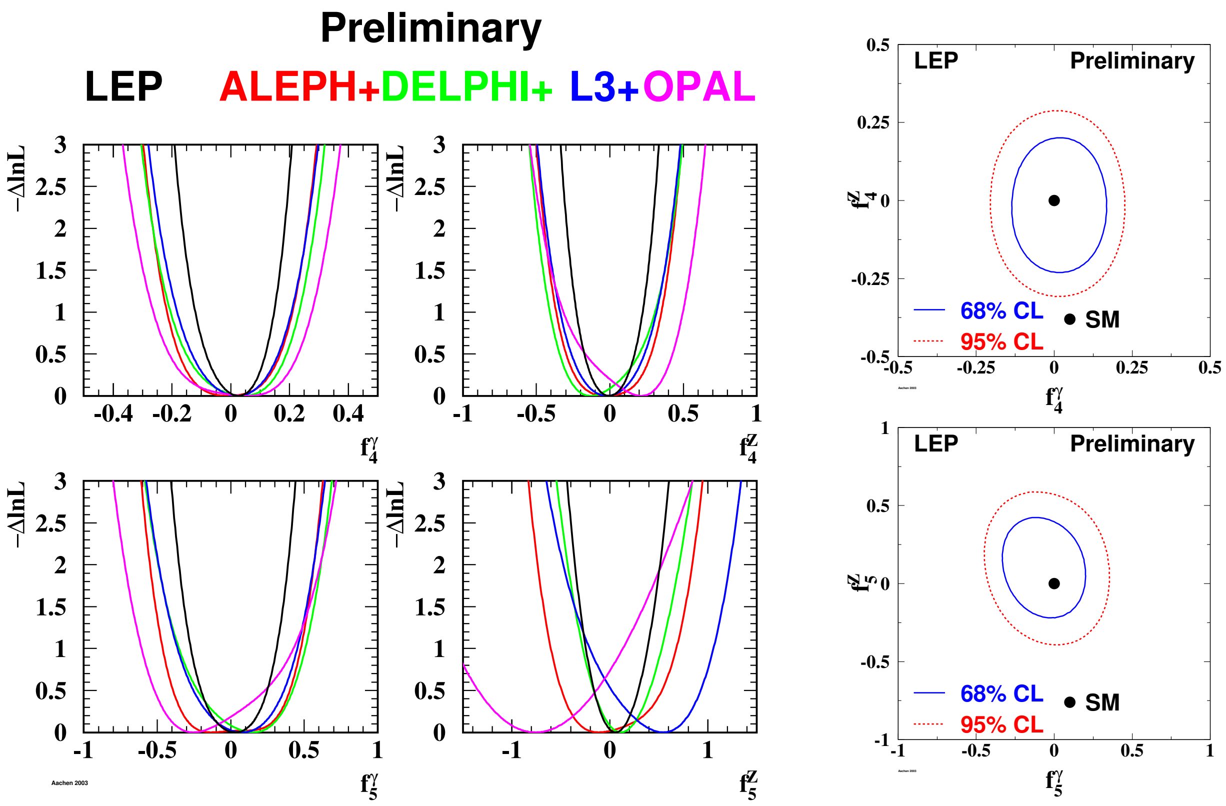

Figure 11: *LEP Log-likelihood curves for the f_i couplings (left plots) and 68% and 95% c.l. contours obtained from two-parameter fits (right plots)*

4 Quartic Gauge Couplings

Since the effect of the SM quartic gauge couplings is negligible at LEP2 energy, only anomalous couplings associated with new effective Lagrangian terms have been studied. Many models with anomalous triple gauge boson couplings predict also the existence of anomalous QGCs. These models have not been considered, since they can be better constrained by their contributions to TGCs. Only genuine QGCs not associated with any contribution to TGCs have been considered.

The only relevant vertices at LEP2 energies are WW$\gamma\gamma$, WWZγ and ZZ$\gamma\gamma$. The following CP-conserving effective Lagrangian terms have been considered [11]:

$$L_6^0 = -\frac{e^2}{16}\frac{a_0}{\Lambda^2}F^{\mu\nu}F_{\mu\nu}\vec{W}^{\alpha}\vec{W}_{\alpha} \tag{2}$$

$$L_6^c = -\frac{e^2}{16}\frac{a_c}{\Lambda^2}F^{\mu\alpha}F_{\mu\beta}\vec{W}^{\beta}\vec{W}_{\alpha}, \tag{3}$$

and the CP-violating term [12],

$$L_6^n = -\frac{e^2}{16}\frac{a_n}{\Lambda^2}\vec{W}_{\mu\alpha}\cdot(\vec{W}_{\nu}\times\vec{W}^{\alpha})F^{\mu\nu}, \tag{4}$$

where $F^{\mu\nu}$ is the electromagnetic field tensor and $\vec{W}_{\alpha}$ is the custodial SU(2) field vector,

$$\vec{W}_{\alpha} = \begin{pmatrix} \frac{1}{\sqrt{2}}(W_{\alpha}^{+} + W_{\alpha}^{-}) \\ \frac{i}{\sqrt{2}}(W_{\alpha}^{+} - W_{\alpha}^{-}) \\ Z_{\alpha}/\cos\theta_w \end{pmatrix} \tag{5}$$

The dimensionless QGCs, a_0, a_c and a_n are divided by Λ^2, where Λ is the unknown scale of new physics. The terms L_6^0 and L_6^c describe WW$\gamma\gamma$ and ZZ$\gamma\gamma$ vertices with the same coupling strength. However, a more general approach [13] suggests different couplings for WW$\gamma\gamma$ and ZZ$\gamma\gamma$. Therefore, the LEP analyses distinguish between the WW$\gamma\gamma$ couplings, a_0^W, a_c^W, and the ZZ$\gamma\gamma$ couplings, a_0^Z and a_c^Z. The term L_6^n describes the WWZγ vertex.

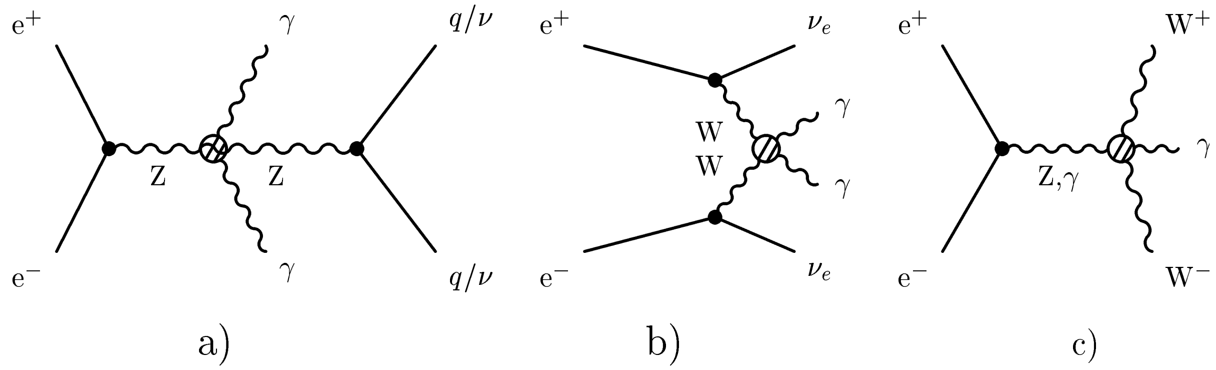

Figure 12: *Feynman diagrams of LEP2 processes with quartic gauge vertices.*

Three processes are used at LEP2 to constrain the QGCs: $e^+e^-\to\nu\bar{\nu}\gamma\gamma$, $e^+e^-\to q\bar{q}\gamma\gamma$ and $e^+e^-\to W^+W^-\gamma$. The Feynman diagrams with quartic gauge vertices associated with these processes are plotted in Fig. 12. Each of the final states can be produced by SM diagrams where the photons are due to initial of final state radiation.

4.1 $\nu\overline{\nu}\gamma\gamma$ Events

The process $e^+e^- \to \nu\overline{\nu}\gamma\gamma$ has been analysed by ALEPH [14], L3 [15] and OPAL [16]. Both diagrams in Figs. 12a and 12b with vertices $ZZ\gamma\gamma$ and $WW\gamma\gamma$ contribute to the $\nu\overline{\nu}\gamma\gamma$ final state. However, in the first diagram the recoil mass against the two photons, namely the $\nu\overline{\nu}$ invariant mass, tends to peak around M_Z, whereas the contribution of the second diagram is distributed almost uniformly over the whole kinematically allowed range. The SM contribution is due to initial state radiation of two photons. The energy spectrum of the least energetic photon, $E_{\gamma 2}$, is sensitive to the contribution of QGCs, since these photons tend to be more energetic for signal events. Using the recoil mass and $E_{\gamma 2}$, it is possible to constrain all four CP-conserving couplings with very little correlation between the $WW\gamma\gamma$ and the $ZZ\gamma\gamma$ couplings.

4.2 $q\overline{q}\gamma\gamma$ Events

The process $e^+e^- \to q\overline{q}\gamma\gamma$ has been analysed by L3 [17]. This process is sensitive only to the $ZZ\gamma\gamma$ couplings (Fig. 12a). The SM contribution is mainly due to initial state radiation. The $q\overline{q}$ invariant mass peaks around M_Z, for both QGC and SM contributions. Like in the case of $\nu\overline{\nu}\gamma\gamma$, the energy spectrum of the least energetic photon has a good sensitivity to any QGC contribution. L3 has also measured the total $q\overline{q}\gamma\gamma$ cross-section for different centre-of-mass energies (see Fig. 13). The cross-section is defined for events where each photon is required to satisfy $E_\gamma > 5$ GeV, $|\cos\theta_\gamma| < 0.97$ and $\cos\theta_{\gamma q} < 0.98$, where $\theta_{\gamma q}$ is the angle between the photon and the nearest jet. In addition, the $q\overline{q}$ invariant mass must be close to M_Z within twice the Z width.

4.3 $W^+W^-\gamma$ Events

The process $e^+e^- \to W^+W^-\gamma$ (Fig. 12c) has been analysed by DELPHI [18], L3 [15] and OPAL [19]. This process is sensitive to the $WW\gamma\gamma$ and $WWZ\gamma$ couplings. Hence it is the only process at LEP2 which can be used to constrain a_n.

The total cross-section is measured within the following acceptance: $E_\gamma > 5$ GeV, $|\cos\theta_\gamma| < 0.95$, $\cos\theta_{\gamma f} < 0.95$ and each W boson must satisfy $|M_{f\overline{f}'} - M_W| < 2\Gamma_W$. Here $\theta_{\gamma f}$ is the angle between the photon and the nearest charged fermion from the W decay, and $M_{f\overline{f}'}$ is the invariant mass of the W decay products. Fig. 13 shows the LEP combined cross-section measurements compared with the theoretical expectations for the SM and for $a_n/\Lambda^2 = 0.1$ and 0.2. The agreement between the data points and SM expectation does not leave much room for any anomalous QGC contribution.

To constrain the QGCs, the differential cross-section as function of the photon polar angle and photon energy is used.

4.4 QGC Results

Since the new physics scale Λ is unknown, all limits are derived for the anomalous coupling divided by Λ^2. The LEP2 results on a_0^W, a_c^W and a_n have not been combined and the 95% c.l. from each individual experiment and each process are listed in Table 4. As can

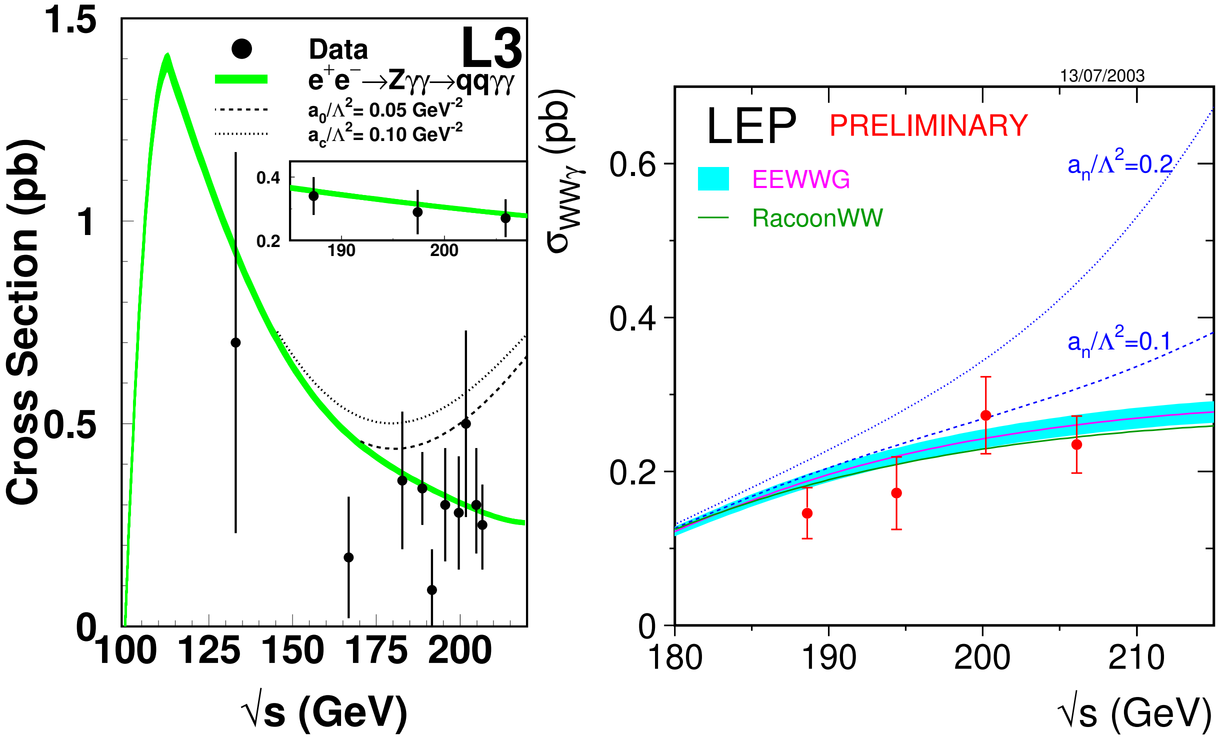

Figure 13: *L3 total* $q\bar{q}\gamma\gamma$ *cross-section (left plot) and combined LEP total* $W^+W^-\gamma$ *cross-section (right plot)*

be seen, the most sensitive process to these QGCs is $e^+e^- \to W^+W^-\gamma$. All results are consistent with zero, namely with the SM. The LEP2 results for a_0^Z and a_c^Z have been combined, and the log-likelihood plots are displayed in Fig. 14 [2]. The corresponding 95% c.l. limits are,

$$
\begin{aligned}
-0.008 < \quad a_0^Z/\Lambda^2 \quad &< 0.021\ \mathrm{GeV}^{-2}, \\
-0.029 < \quad a_c^Z/\Lambda^2 \quad &< 0.039\ \mathrm{GeV}^{-2}.
\end{aligned}
$$

Experiment	Process	a_0^W/Λ^2	a_c^W/Λ^2	a_n/Λ^2
ALEPH	$\nu\bar{\nu}\gamma\gamma$	[-0.060, 0.055]	[-0.099, 0.093]	
DELPHI	$W^+W^-\gamma$	[-0.020, 0.020]	[-0.063, 0.032]	[-0.18, 0.14]
L3	$\nu\bar{\nu}\gamma\gamma$	[-0.031, 0.031]	[-0.090, 0.090]	
	$W^+W^-\gamma$	[-0.017, 0.017]	[-0.052, 0.026]	[-0.14, 0.13]
OPAL	$\nu\bar{\nu}\gamma\gamma$	[-0.054, 0.052]	[-0.15, 0.14]	
	$W^+W^-\gamma$	[-0.020, 0.020]	[-0.053, 0.037]	[-0.16, 0.15]

Table 4: 95% c.l. limits on charged current QGCs in GeV^{-2} obtained by the four LEP experiments.

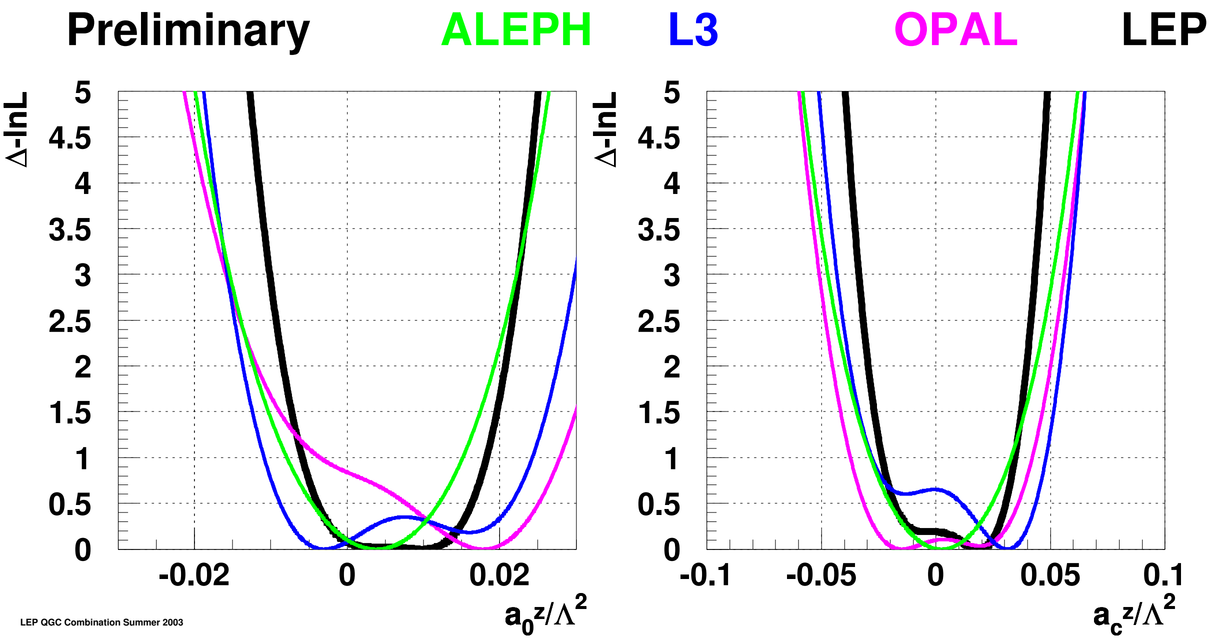

Figure 14: *LEP Log-likelihood curves for the neutral current QGCs*

5 Summary

The four LEP experiments have measured the charged current triple gauge couplings using W-pairs, single W and single photon events. The precision achieved is 0.02 for Δg_1^z and λ, and 0.045 for $\Delta\kappa_\gamma$. Constraints have been set on anomalous neutral current triple gauge couplings and on quartic gauge couplings. Not all the LEP results are final, but significant improvement in precision is not expected. All anomalous couplings are consistent with zero and no statistical significant deviation from the SM is observed.

I wish to thank the QFTHEP'2003 organisers for their assistance before, during and after the conference. I am grateful also to my colleagues in OPAL and to U. Parzefall for their cooperation.

References

[1] Physics at LEP2, edited by G. Altarelli *et al.*, CERN 96-01 Vol. 1, 525, and references therein.

[2] The LEP Collaborations ALEPH, DELPHI, L3, OPAL, the LEP Electroweak Working group and the SLD Heavy Flavour Group, "A Combination of Preliminary Electroweak Measurements and Constants on the Standard Model", CERN-EP/2003-XXX, and references therein. `http://arXiv.org/abs/hep-ex/0312023`

[3] S. Jadach *et al.*, Comp. Phys. Comm. **140** (2001) 432.

[4] A. Denner *et al.*, Nucl. Phys. **B587** (2000) 67.

[5] OPAL Collaboration, G. Abbiendi *et al.*, CERN-EP/2003-042, July 2003, submitted to Eur. Phys. J. C.

[6] ALEPH Collaboration, ALEPH Note, ALEPH 2003-015, CONF 2003-011, July 2003.

[7] OPAL Collaboration, G. Abbiendi *et al.*, Eur. Phys. J. **C19** (2001) 229.

[8] G. J. Gounaris, J. Layssac and F. Renard, Phys. Rev. **D62** (2000) 073013

[9] K. Hagiwara *et al.*, Nucl. Phys. **B282** (1987) 253

[10] DELPHI Collaboration, DELPHI Note, DELPHI 2001-097, CONF 525, July 2001.

[11] G. Bélanger and F. Boudjema, Phys. Lett. **B288** (1992) 201.

[12] W. J. Stirling and A. Werthenbach, Eur. Phys. J. **C14** (2000) 103.

[13] G. Bélanger *et al.*, Eur. Phys. J. **C13** (2000) 283

[14] ALEPH Collaboration, ALEPH Note, ALEPH 2003-009, CONF 2003-006, June 2003.

[15] L3 Collaboration, P. Achard *et al.*, Phys. Lett. **B527** (2002) 29.

[16] OPAL Collaboration, OPAL Physics Note, PN510, July 2002.

[17] L3 Collaboration, P. Achard *et al.*, Phys. Lett. **B540** (2002) 43.

[18] DELPHI Collaboration, DELPHI Note, DELPHI 2003-059, CONF 679, June 2003.

[19] OPAL Collaboration, G. Abbiendi *et al.*, CERN-EP/2003-043, July 2003, submitted to Phys. Lett. B.